Wireless Personal Communications **12:** 175–186, 2000.

Analysis of the Effect of the I/Q Base-Band Filter Mismatch in an OFDM Modem *

MARIA-GABRIELLA DI BENEDETTO and PAOLO MANDARINI
Università degli Studi di Roma "La Sapienza", Dipartimento INFOCOM, via Eudossiana, 18, 00184 Rome, Italy
E-mail: gaby@acts.ing.uniroma1.it

Abstract. In digital communication modems in which a very high rate system clock is used, it is necessary to use analog base-band shaping filters in the inphase (I) and quadrature (Q) paths of the modulator. However, this type of implementation inherently produces a mismatch of the I and Q paths. In the present paper, results of the analysis of the transmitter (TX) I/Q mismatch in an Orthogonal Frequency Division Multiplexing (OFDM) system with Differential Coherent Quadrature Phase Shift Keying (DQPSK) modulation is presented. Theoretical analysis shows that the Signal-to-Noise (SNR) degradation due to the I/Q mismatch can be represented by a mismatch transfer function on the basis of which one can compute the maximum affordable amplitude and phase mismatch of the TX filters transfer functions.

Keywords: modulation, OFDM, analog filters.

1. Introduction

In Orthogonal Frequency Division Multiplexing (OFDM) systems [1, ch. 15] which use Differential Quadrature Phase Shift Keying (DQPSK), the reference axis for each submodulator in the frequency domain is derived from the phase of the previous (in frequency) submodulator. This scheme is used in "burst mode" transmissions, in which previous (in time) OFDM symbols can be used by different users. Such a specification characterizes the physical layer of the MEDIAN system [2] under development in the MEDIAN project, which belongs to the European Community ACTS program. The present work represents part of a larger investigation carried out at the University of Rome "La Sapienza" on the transmission aspects of MEDIAN [3, 4]. MEDIAN is a system to be designed for multimedia communications in a Wireless Local Area Network (WLAN); it operates in the 60 GHz band and uses data rates up to 300 Mbits/sec. Due to this very high data-rate, analog base-band (BB) shaping filters must be used on the inphase (I) and quadrature (Q) paths. The present paper analyzes the degradation produced by the transmitter (TX) I-Q filters mismatch on system performance. The above degradation is described by a mismatch transfer function from which one can compute the maximum affordable amplitude and phase mismatch of the TX filters transfer functions, as a function of a required system performance. The paper is organized as follows; Section 2 describes the modem operations of a full-digital QPSK/OFDM modem. In Section 3, the add-on necessary to realize a differential scheme (DQPSK/OFDM) are reported, and the error probability is evaluated. In Section 4, the effects of the I/Q mismatch are examined on a theoretical basis. Finally, Section 5 contains the application of the analysis, and Section 6 the conclusions.

* This paper was presented in part at the 1996 ACTS Mobile Telecommunications Summit, Granada, Nov. 27–29, 1996.

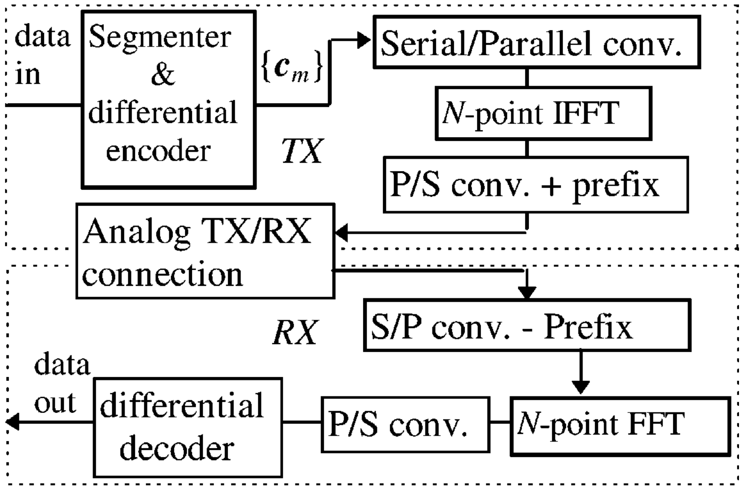

Figure 1. Block diagram of an OFDM modem.

2. Description of a QPSK-OFDM Modem

In Orthogonal Frequency Division Multiplex the different data sequences are first digitally modulated and then frequency multiplexed. Each submodulator uses the same modulation (QAM, PSK, etc.), the same symbol period T_s, the same rectangular data pulse, and carries β bits/symbol. The carrier frequencies of the submodulators, called subcarriers, are spaced by Δf around the system carrier frequency f_p; moreover, T_s must be greater than $T_o = 1/\Delta f$, and is usually written as $T_s = T_o + T_g$. T_g is a guard time which is introduced to cope with defective symbol synchronization and multipath. Other important parameters of the OFDM modem are the number N of available subcarriers (a power of two) and the number $N_u = M_1 + M_2 < N$ of effectively used subcarriers (M_1 is the number of subcarriers at frequencies above the system carrier, $M_2 - 1$ is the number of subcarriers below the system carrier). The energy spectrum of an OFDM signal is roughly bandlimited to $B = N \cdot \Delta f$. The frequency of the system clock is thus B. A full-digital implementation of the OFDM scheme, based on the use of IFFT/FFT processors ([5, 6], Figure 1), produces a sequence of $N + N_g$ complex samples for each OFDM symbol; N samples belong to T_o while $N_g = T_g \cdot B$ samples form the prefix. The above samples are Digital-To-Analog converted (DAC), modulated, and sent over an analog connection. Figure 2 represents the BB equivalent of the overall connection, in which the mismatch between the TX I-Q paths is highlighted. The analog filters are indicated by $\boldsymbol{H}_{BTI}(f)$ and $\boldsymbol{H}_{BTQ}(f)$, for the I and Q paths, respectively, while ϕ represents the phase error between the I and Q carriers.

In a QPSK-OFDM system, the complex envelope of the transmitted signal, $\boldsymbol{x}(t)$, is generated by an IFFT processor from a sequence of $N_u < N$ constellation points $\{\boldsymbol{c}_{-M_2-1}, .., \boldsymbol{c}_0, .., \boldsymbol{c}_{M_1}\}$. The sequence $\{\boldsymbol{c}_m\}$ is generated by a segmenter and differential encoder, from the input binary data sequence (see Figure 1). Referring to Figure 2, the complex envelope of the signal at the output of the DAC, and its Fourier Transform (FT) are given by

$$\boldsymbol{x}(t) = \sum_{k=-N_g}^{N-1} \boldsymbol{d}_k \cdot \mathrm{rect}(t - k/B) \quad \text{and} \quad \boldsymbol{X}(f) = \Xi(f) \cdot \sum_{k=-N_g}^{N-1} \boldsymbol{d}_k \cdot \boldsymbol{e}^{-j2\pi f k/B}, \tag{1}$$

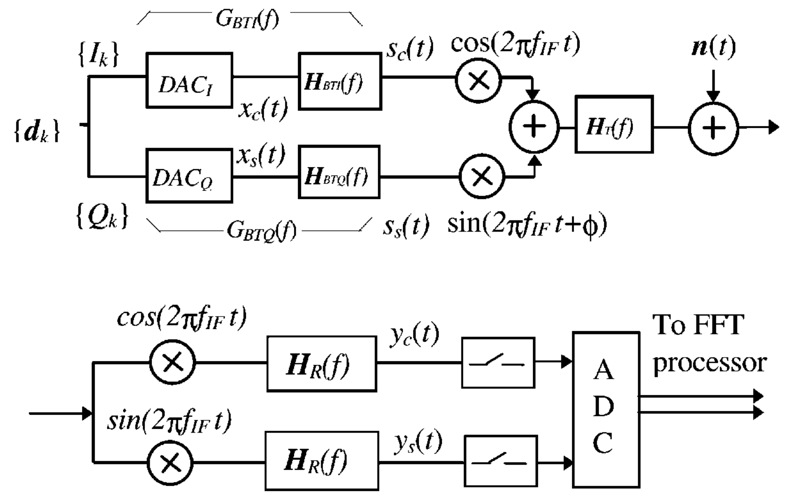

Figure 2. Block diagram of the baseband equivalent of the analog TX/RX connection.

where

$$\mathrm{rect}(t) \equiv \begin{cases} 1 & -1/2B \le t < 1/2B \\ 0 & \text{elsewhere} \end{cases} \Leftrightarrow \Xi(f) \equiv \frac{1}{B}\frac{\sin(\pi f/B)}{\pi f/B} \tag{2}$$

$$\boldsymbol{d}_k = \text{IFFT of } \{\boldsymbol{D}_m\} \text{ periodic of period } N; \quad \boldsymbol{D}_m = \begin{cases} \boldsymbol{c}_m & 0 \le m \le M_1 \\ 0 & M_1 < m \le N - M_2 \\ \boldsymbol{c}_{m-N} & N - M_2 < m \le N - 1 \end{cases} \tag{3}$$

In the present section, the I and Q paths are supposed to be identical. Thus, one has

$$\boldsymbol{H}_{BTI}(f) = \boldsymbol{H}_{BTQ}(f) \equiv \boldsymbol{H}_{BT}(f) \tag{4}$$

and ϕ, the phase mismatch between the channels, is zero.

Therefore, the received complex envelope after demodulation and filtering, $\boldsymbol{y}(t)$, and its Fourier Transform, $\boldsymbol{Y}(f)$, are given by

$$\boldsymbol{y}(t) = \sum_{k=-N_g}^{N-1} \boldsymbol{d}_k \cdot \boldsymbol{g}(t - k/B) \Leftrightarrow \boldsymbol{Y}(f) = \boldsymbol{G}(f) \cdot \sum_{k=-N_g}^{N-1} \boldsymbol{d}_k \cdot e^{-j2\pi f \frac{k}{B}}, \tag{5}$$

where

$$\boldsymbol{g}(t) \Leftrightarrow \boldsymbol{G}(f) = \frac{1}{B}\frac{\sin(\pi f/B)}{\pi f/B} \cdot \boldsymbol{H}_{BT}(f) \cdot \boldsymbol{H}_T(f) \cdot \boldsymbol{H}_R(f) \equiv \frac{1}{B}\boldsymbol{G}_T(f) \cdot \boldsymbol{H}_R(f). \tag{6}$$

In (6), $H_T(f)$ is the transfer function of the IF-RF TX filter, and $H_R(f)$ is the transfer function of the low-pass receiving filter. $\boldsymbol{y}(t)$ is sampled at frequency $B = N \cdot \Delta f$. If the duration of $\boldsymbol{g}(t)$ is lower than T_g, it can be derived (see Appendix A) that the m-th FFT output, i.e. an estimate of the transmitted constellation point $\boldsymbol{c}_m$, is given by

$$\boldsymbol{c}_m^{\wedge} = \boldsymbol{G}_T(m \cdot \Delta f) \cdot \boldsymbol{H}_R(m \cdot \Delta f) \cdot \boldsymbol{c}_m = B \cdot \boldsymbol{G}(m \cdot \Delta f) \cdot \boldsymbol{c}_m, \quad -M_2 < m \le M_1 .$$

Therefore, the estimate of $\boldsymbol{c}_m$ is biased by a complex factor $B \cdot \boldsymbol{G}(m \cdot \Delta f)$. In a coherent scheme, the amplitude of this factor may be irrelevant, while its phase may destroy the information. As it is well known, this can be avoided by using a differentially coherent scheme.

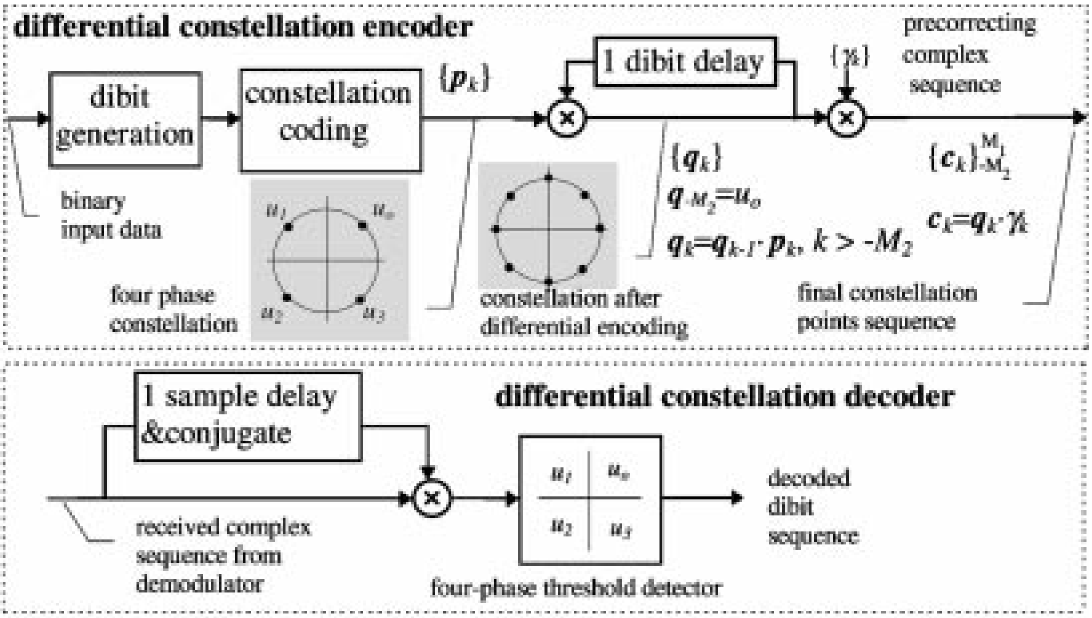

Figure 3. Block diagram of the differential co/decoder.

3. Error Probability in a DQPSK/OFDM System on the AWGN Channel

On the Additive White Gaussian Noise (AWGN) channel a complex zero-mean gaussian process $\boldsymbol{n}(t)$, with two-sided power spectrum $P_N(f) = 4N_o$ is added to the complex envelope of the received signal $\boldsymbol{y}(t)$, where $\boldsymbol{N}_o$ is the two-sided power density of the noise added to the modulated signal. The noise produces an additive zero-mean gaussian complex noise sample $\boldsymbol{n}_k$ on each FFT output, with variance given by ([5])

$$\psi_m^2 = \frac{B}{N} P_N(m \cdot \Delta f) = 4N_0 |\boldsymbol{H}_R(f_m)|^2 \Delta f. \tag{7}$$

The data sequence is grouped into dibits and coded using QPSK, as shown in Figure 3, to produce a sequence $\{\boldsymbol{p}_k\}$ which is then differentially encoded to generate a sequence $\{\boldsymbol{q}_k\}$, such that $\boldsymbol{q}_{m-1}^* \cdot \boldsymbol{q}_m = \boldsymbol{p}_m$. The elements of the sequence $\{\boldsymbol{q}_k\}$ are points of an 8-phase constellation, i.e. complex values which are equally-spaced and with unitary modulus. Each $\boldsymbol{q}_k$, is then multiplied by a precorrection factor $\gamma_k = 1/\boldsymbol{G}_T(f_k)$ which equalizes the amplitude of each subcarrier, to produce the transmitted constellation sequence $\boldsymbol{c}_k = \boldsymbol{q}_k/\boldsymbol{G}_T(f_k)$. Therefore, the received signal power, which is half the power of its complex envelope, is given by

$$P_R \cong \frac{1}{2} \sum_{k=-M_2}^{M_1} |\gamma_k|^2 |\boldsymbol{G}_T(f_k)|^2 = \frac{N_u}{2}. \tag{8}$$

Finally, *SNR* indicates the ratio between the received power and the noise power in a frequency band equal to the on-air symbol rate, which is given by

$$f_s = N_u/T_s = N_u/[T_o(1 + T_g/T_o)] = N_u \Delta f/(1 + T_g/T_o).$$

From (8), one has

$$SNR = \frac{P_R}{2N_o f_s} = (1 + T_g/T_o) \frac{1}{4N_o \Delta f}. \tag{9}$$

If differential co/decoding is taken into account, the estimate of the transmitted constellation point $\boldsymbol{p}_m$ is

$$\begin{aligned} \boldsymbol{p}_m^{\wedge} &= \boldsymbol{c}_{m-1}^{\wedge *}\boldsymbol{c}_m^{\wedge} = \{\boldsymbol{H}_R^*(f_{m-1})\cdot \boldsymbol{q}_{m-1}^* + \boldsymbol{n}_{m-1}^*\}\{\boldsymbol{H}_R(f_m)\cdot \boldsymbol{q}_m + \boldsymbol{n}_m\} \\ &\cong \boldsymbol{H}_R^*(f_{m-1})\cdot \boldsymbol{H}_R(f_m)\cdot \boldsymbol{p}_m + \boldsymbol{H}_R(f_m)\cdot \boldsymbol{q}_m \cdot \boldsymbol{n}_{m-1}^* + \boldsymbol{H}_R^*(f_{m-1})\cdot \boldsymbol{q}_{m-1}^*\cdot \boldsymbol{n}_m \\ &\equiv \beta_m \boldsymbol{p}_m + \nu_m \,. \end{aligned} \tag{10}$$

Equation (10) shows that the estimate of $\boldsymbol{p}_m$ is affected by an additive gaussian noise component ν_m and by a multiplicative bias $\beta_m = \boldsymbol{H}_R^*(f_{m-1})\cdot \boldsymbol{H}_R(f_m) \equiv b_m \cdot e^{j\varphi_m}$, as in a coherent system. However, in the present case, φ_m is small since it is the phase difference of $\boldsymbol{H}_R(f)$ values computed at frequencies spaced by Δf. Since $\boldsymbol{n}_m$ and $\boldsymbol{n}_{m-1}$ are independent and since $|\boldsymbol{q}_m| = 1$, the variance of ν_m is, from (10)

$$\sigma_\nu^2 = (|\boldsymbol{H}_R(f_m)|^2 + |\boldsymbol{H}_R(f_{m-1})|^2)\cdot 4N_o|\boldsymbol{H}_R(f_m)|^2\Delta f.$$

Finally, since $\boldsymbol{p}_m = (\pm 1 \pm j)/\sqrt{2}$, the bit error rate on the m-th constellation point is (see Appendix B)

$$\begin{aligned} P_m &= \frac{1}{4}erfc(z_{m+}) + \frac{1}{4}erfc(z_{m-}) \\ z_{m\pm}^2 &= \left\{\frac{b_m(\cos\varphi_m \pm \sin\varphi_m)}{\sqrt{2}\sigma_\nu}\right\}^2 = \frac{|\boldsymbol{H}_R(f_{m-1})|^2\cdot(\cos\varphi_m \pm \sin\varphi_m)^2}{8N_o\Delta f\{|\boldsymbol{H}_R(f_m)|^2 + |\boldsymbol{H}_R(f_{m-1})|^2\}} \cong \\ &= \frac{(\cos\varphi_m \pm \sin\varphi_m)^2}{16N_o\Delta f} = \frac{SNR\cdot(\cos\varphi_m \pm \sin\varphi_m)^2}{4(1+T_g/T_o)} \,. \end{aligned} \tag{11}$$

4. Effect of LP Transmitter Filters Mismatch on the I and Q Paths

In Figure 2, the input sequence is represented by two real sequences $\{I_k\}$ and $\{Q_k\}$ which are D to A converted, filtered and cos/sin modulated. We indicate by

$$\begin{aligned} \boldsymbol{G}_{BTI}(f) &\equiv \frac{\sin(\pi f/B)}{B\cdot \pi f/B}\boldsymbol{H}_{BTI}(f)\cdot \boldsymbol{H}_T(f) \\ \boldsymbol{G}_{BTQ}(f) &\equiv \frac{\sin(\pi f/B)}{B\cdot \pi f/B}\boldsymbol{H}_{BTQ}(f)\cdot \boldsymbol{H}_T(f) \end{aligned} \tag{12}$$

the equivalent low-pass filters of the I and Q paths, respectively, at the TX side. The RF signal can be represented by

$$\begin{aligned} & s(t) = s_c(t)\cdot\cos(2\pi f_p t) - s_s(t)\cdot\sin(2\pi f_p t + \phi) \equiv s_I(t)\cdot\cos(2\pi f_p t) - s_Q(t)\cdot\sin(2\pi f_p t) \\ & s_I(t) \equiv s_c(t) - \sin\phi\cdot s_s(t) \\ & s_Q(t) \equiv \cos\phi\cdot s_s(t) \\ & s_c(t) = \textstyle\sum_{k=-N_g}^{N-1} I_k g_{BTI}(t-k/B) \\ & s_s(t) = \textstyle\sum_{k=-N_g}^{N-1} Q_k g_{BTQ}(t-k/B) \end{aligned} \tag{13}$$

or by the Fourier Transform of its complex envelope $\boldsymbol{s}(t) = s_I(t) + j\cdot s_Q(t)$

$$\begin{aligned} \boldsymbol{S}(f) = {} & F\{s_I(t) + js_Q(t)\} = \\ & \boldsymbol{G}_{BTI}(f)\textstyle\sum_{k=-N_g}^{N-1} I_k e^{-j2\pi fk/B} + je^{j\phi}\boldsymbol{G}_{BTQ}(f)\sum_{k=-N_g}^{N-1} Q_k e^{-j2\pi fk/B} \,. \end{aligned} \tag{14}$$

Define

$$\begin{aligned}\boldsymbol{G}_T(f) &\equiv \frac{B}{2}\{\boldsymbol{G}_{BTI}(f) + e^{j\phi}\boldsymbol{G}_{BTQ}(f)\}\\ \boldsymbol{G}_e(f) &\equiv \frac{B}{2}\{\boldsymbol{G}_{BTI}(f) - e^{j\phi}\boldsymbol{G}_{BTQ}(f)\}\,.\end{aligned} \tag{15}$$

Then

$$\begin{aligned}\boldsymbol{S}(f) &= \frac{1}{B}\left\{\boldsymbol{G}_T(f)\cdot\sum_{k=-N_g}^{N-1}(I_k + jQ_k)\cdot e^{-j2\pi fk/B} + \boldsymbol{G}_e(f)\cdot\sum_{k=-N_g}^{N-1}(I_k - jQ_k)\cdot e^{-j2\pi fk/B}\right\} = \\ &= \frac{1}{B}\left\{\boldsymbol{G}_T(f)\cdot\sum_{k=-N_g}^{N-1}\boldsymbol{d}_k\cdot e^{-j2\pi fk/B} + \boldsymbol{G}_e(f)\cdot\sum_{k=-N_g}^{N-1}\boldsymbol{d}_k^* e^{-j2\pi fk/B}\right\}\,.\end{aligned} \tag{16}$$

Equation (16) shows that the I-Q TX mismatch adds a conjugate component to the transmitted sequence. Therefore, the m-th outputs of the FFT processor due to the first and second component in (16), are given by[1]

$$\boldsymbol{c}_m^{\wedge(I)} = \boldsymbol{H}_R(f_m)\cdot\boldsymbol{G}_T(f_m)\cdot\boldsymbol{c}_m = \boldsymbol{H}_R(f_m)\cdot\boldsymbol{G}_T(f_m)\cdot\gamma_m\cdot\boldsymbol{q}_m \tag{17}$$

$$\boldsymbol{c}_m^{\wedge(Q)} = \boldsymbol{H}_R(f_m)\cdot\boldsymbol{G}_e(f_m)\cdot\boldsymbol{c}_{-m}^* = \boldsymbol{H}_R(f_m)\cdot\boldsymbol{G}_e(f_m)\cdot\gamma_{-m}^*\cdot\boldsymbol{q}_{-m}^*\,. \tag{18}$$

Under the ideal choice[2] $\gamma_k = 1/\boldsymbol{G}_T(f_k) = \gamma_{-k}^*$, and since the demodulation process is linear, the m-th output is

$$\begin{aligned}\boldsymbol{c}_m^{\wedge} &= \boldsymbol{c}_m^{\wedge(i)} + \boldsymbol{c}_m^{\wedge(Q)} = \boldsymbol{H}_R(f_m)\cdot\left(\boldsymbol{q}_m + \frac{\boldsymbol{G}_e(f_m)}{\boldsymbol{G}_T(f_m)}\cdot\boldsymbol{q}_{-m}^*\right)\\ &\equiv \boldsymbol{H}_R(f_m)\cdot(\boldsymbol{q}_m + \boldsymbol{H}_e(f_m)\cdot\boldsymbol{q}_{-m}^*)\end{aligned} \tag{19}$$

where

$$\boldsymbol{H}_e(f_m) \equiv \frac{\boldsymbol{G}_e(f)}{\boldsymbol{G}_T(f)} = \frac{\boldsymbol{G}_{BTI}(f) - e^{j\phi}\boldsymbol{G}_{BTQ}(f)}{\boldsymbol{G}_{BTI}(f) + e^{j\phi}\boldsymbol{G}_{BTQ}(f)} \equiv a_m e^{j\mu_m}\,. \tag{20}$$

$\boldsymbol{H}_e(f_m)$ is called mismatch transfer function and is responsible for the interference induced by the TX I-Q mismatch. As a matter of fact, $\boldsymbol{H}_e(f_m) = 0$ if the mismatch is absent ($\phi = 0$ and $G_{BTI}(f) = G_{BTQ}(f)$). Moreover, Equation (19) shows that any TX mismatch causes an additive error component on a transmitted constellation point $\boldsymbol{q}_m$ which depends upon $\boldsymbol{q}_{-m}^*$ through $\boldsymbol{H}_e(f_m)$. Note that $\boldsymbol{H}_e(f_m)$ does not depend upon the IF-RF TX filters. After differential decoding, in absence of noise and for $|\boldsymbol{H}_e(f_m)| \ll 1$, one has

$$\begin{aligned}\boldsymbol{p}_m^{\wedge} &= \boldsymbol{c}_{m-1}^{\wedge *}\boldsymbol{c}_m^{\wedge} = \boldsymbol{H}_R^*(f_{m-1})\boldsymbol{H}_R(f_m)\{\boldsymbol{q}_{m-1}^* + \boldsymbol{H}_e^*(f_{m-1})\cdot\boldsymbol{q}_{-m-1}\}\cdot\{\boldsymbol{q}_m + \boldsymbol{H}_e(f_m)\cdot\boldsymbol{q}_{-m}^*\}\\ &\cong \boldsymbol{H}_R^*(f_{m-1})\boldsymbol{H}_R(f_m)\{\boldsymbol{p}_m + \boldsymbol{H}_e(f_m)\cdot\varepsilon_m + \boldsymbol{H}_e^*(f_{m-1})\cdot\eta_m\} \equiv \beta_m\boldsymbol{p}_m + \alpha_m\,,\end{aligned} \tag{21}$$

where $\varepsilon_m \equiv \boldsymbol{q}_{m-1}^*\boldsymbol{q}_{-m}^* = e^{j\vartheta_m}$ and $\eta_m \equiv \boldsymbol{q}_m\boldsymbol{q}_{-m-1} = e^{j\theta_m}$ with phases ϑ_m and θ_m which take 8 different values, uniformly distributed along the round angle. Equation (21) shows that the estimate of $\boldsymbol{p}_m$ is affected by a multiplicative complex bias β_m and by an additive complex

---

[1] Note that $\sum_{k=0}^{N-1}\boldsymbol{d}_k^* e^{-j2\pi nm/N} = (\sum_{k=0}^{N-1}\boldsymbol{d}_k e^{j2\pi nm/N})^* = \boldsymbol{D}_{-m}^* = \boldsymbol{D}_{N-m}^*$.

[2] We have supposed that the IF/RF transmitting filters have arithmetic symmetry around the carrier frequency.

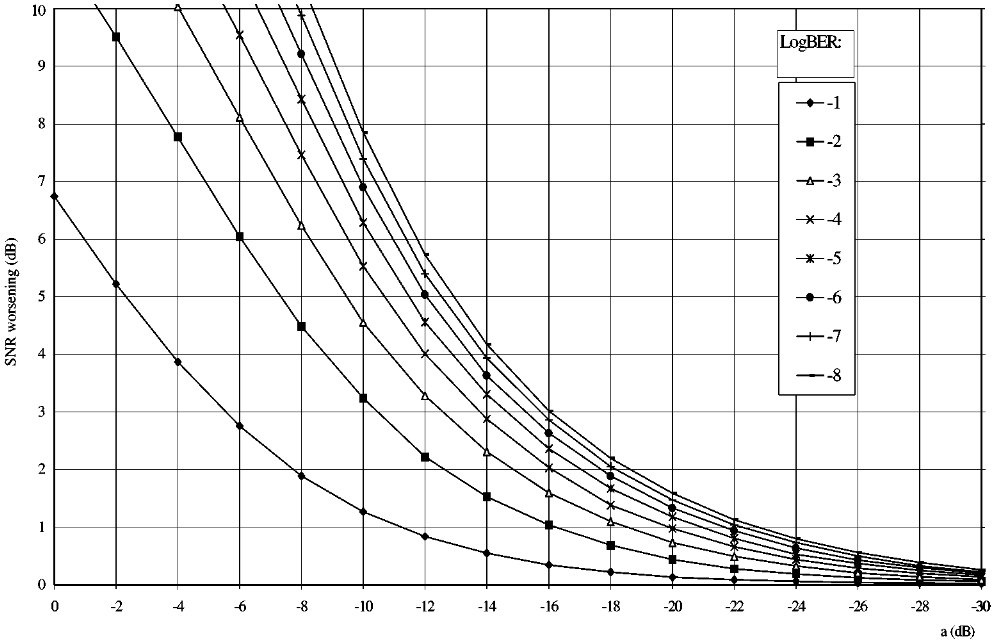

Figure 4. SNR degradation versus a (dB), for different values of $\log_{10}$(Bit Error Probability) evaluated @ $a = 0$.

bias α_m. By applying the same procedure as shown in Section 2, each bit-decision on the m-th transmitted constellation point is affected by the following bit error probability

$$\begin{aligned} P_m(\psi_m, \zeta_m) &= \frac{1}{4} erfc(z_{m+}) + \frac{1}{4} erfc(z_{m-}) \\ z_{m\pm}^2 &= \frac{SNR}{4(1 + T_g/T_o)} [1 \pm \sqrt{2} a_m (\cos \omega_m + \cos \zeta_m)]^2 , \end{aligned} \tag{22}$$

where

$$\begin{aligned} &\omega_m = \vartheta_m + \mu_m \quad \zeta_m = \theta_m - \mu_m \\ &a_m = |\boldsymbol{H}_e(f_m)| \quad \mu_m = \mathrm{Arg}\{\boldsymbol{H}_e(f_m)\} \quad \text{(see Equation (20))}. \end{aligned}$$

Finally, the mean error probability can be obtained by averaging (22) over ω_m and ζ_m, which can be assumed as random variables uniformly distributed over 0-2π, given the hypothesis on θ_m and ϑ_m. Figure 4 shows the SNR degradation due to the presence of the mismatch between the I and Q paths, represented by the corresponding value of $a_m = a_{\mathrm{dB}}$ (dB) and for different values of the error probability, evaluated for $a_{\mathrm{dB}} = 0$. We conclude that, for example, if 1 dB SNR degradation is accepted for each used subcarrier, the maximum value of a_{dB} is –23 dB.

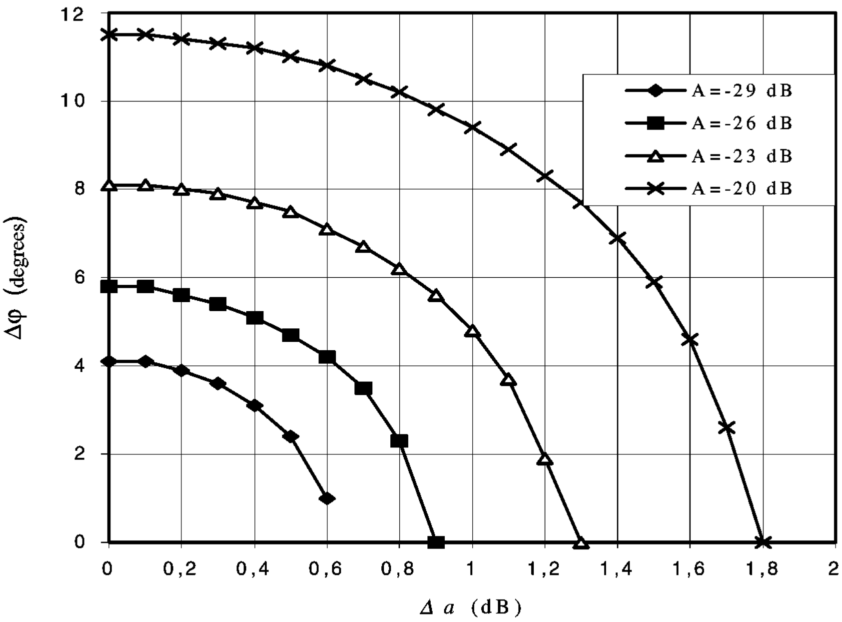

Figure 5. Locus of the points, in the plane $\{\Delta a_{(\mathrm{dB})}, \Delta\varphi_{(\mathrm{degree})}\}$ for which $20\,\log_{10} a < A_{\mathrm{dB}}$.

5. Applications

5.1. Maximum Amplitude/Phase Mismatch Between the In-Phase and in Quadrature Filters

The effect of the amplitude/phase mismatch between the inphase and quadrature LP transmitter filters can be isolated by supposing the perfect orthogonality between che inphase and quadrature carriers (i.e. $\varphi = 0°$). In this case, indicating by $a = |\boldsymbol{H}_e(f)|$, one has, from (20):

$$a = \left| \frac{1 - \Delta a_{BT}(f) \cdot e^{j\Delta\varphi_{BT}(f)}}{1 + \Delta a_{BT}(f) \cdot e^{j\Delta\varphi_{BT}(f)}} \right| ,$$

with

$$\Delta a_{BT}(f) \equiv |\boldsymbol{G}_{BTQ}(f)/\boldsymbol{G}_{BTI}(f)|$$
$$\Delta\varphi_{BT}(f) \equiv \arg\{\boldsymbol{G}_{BTQ}(f)/\boldsymbol{G}_{BTI}(f)\} .$$

Figure 5 shows the area in the $\{\Delta a_{(\mathrm{dB})}, \Delta\varphi_{(\mathrm{degree})}\}$ plane for which $20\,\log_{10} a < A_{\mathrm{dB}}$. For example, note that corresponding to $A_{\mathrm{dB}} = -23$ dB, a maximum phase mismatch of 8° is possible only in the presence of perfect amplitude matching ($\Delta a = 0$ dB); the phase mismatch allowed is reduced to zero for an amplitude mismatch of 1.3 dB.

5.2. Effect of the Phase Error ϕ Between the In-Phase and In-Quadrature Transmitter Carriers

The effect of a phase error ϕ between the inphase and quadrature transmitter carriers can be isolated by supposing $\boldsymbol{G}_{BTI}(f) = \boldsymbol{G}_{BTQ}(f)$. One obtains

$$a_{\mathrm{dB}} \equiv 20 \log_{10} |\boldsymbol{H}_e(f)| = 20 \log_{10} \left| \frac{1 - e^{j\phi}}{1 + e^{j\phi}} \right| . \tag{23}$$

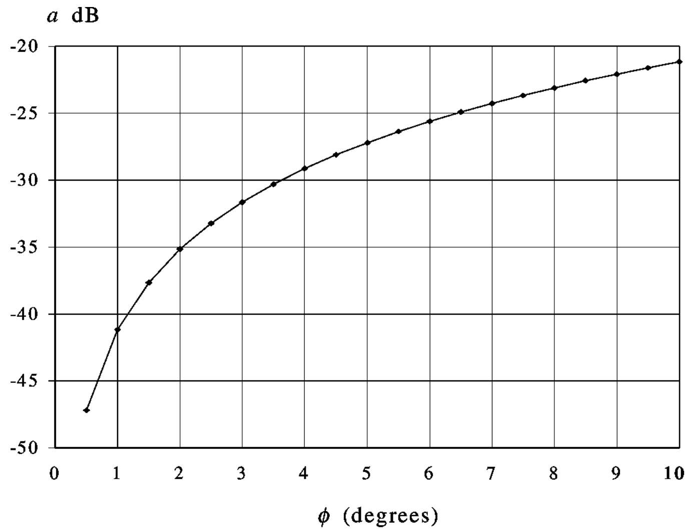

Figure 6. Behavior of a_{dB} versus φ.

Figure 6 represents the behavior of a_{dB} versus ϕ. Figures 4 and 6 can be used jointly: when a degradation of 1 dB on SNR is imposed @ BER $= 10^{-8}$, it appears from Figure 4 that $a = -23$ dB and from Figure 6 the maximum phase error must be 8°.

6. Conclusions

In this paper, the effects of a mismatch between the I and Q transmitter paths in a DQPSK-OFDM modem were examined. It was shown that the worsening effects of the mismatch can be taken into account by a mismatch function $\boldsymbol{H}_e(f)$, which must be limited for any accepted SNR degradation. On the basis of theoretical considerations, the maximum amplitude/phase mismatcth of the BB filters in the transmitter's LP paths and the maximum phase error of the inphase and quadrature carriers were determined.

Future work will include mismatch effects on the receiver side.

Acknowledgements

This work was partly funded by the European Community in the framework of the project ACTS AC006 Median.

References

1. W.T. Webb and L. Hanzo: *Modern Quadrature Amplitude Modulation*, Pentech Press: London, 1994.
2. European Community ACTS MEDIAN project AC006, "Wireless Broadband CPN/LAN for Professional and Residential Multimedia Applications", Final System Design, Deliverable MD3, CEC reference#AC006/MED/PAR/DS/R/054/b1, December 1996.
3. M.G. Di Benedetto and P. Mandarini, "An Application of the MMSE Predistortion to OFDM Systems", *IEEE Trans. Communications*, Vol. 44, No. 11, pp. 1417–1420, 1996.
4. P. Mandarini, M.G. Di Benedetto, R. Lelouarn, V. Brankovic and T. Dequen, "Analysis of Non-Linearities in the Median System", in *Proc. Acts Mobile Telecommunications Summit*, Granada, Spain, 1996, pp. 446–449.

5. T. de Couasnon, R. Monnier and J.B. Rault, "OFDM for Digital TV Broadcasting", Signal processing 39 I-32, pp. 1–32, 1994.
6. B. le Floch, M. Alard and C. Berrou, "Coded Orthogonal Frequency Division Multiplex", in *Proc. IEEE*, Vol. 83, No. 6, pp. 982–996, 1995.

Appendix A

The sequence $\boldsymbol{d}_k$ is periodic of period N: therefore, the signal $\boldsymbol{x}_o(t)$:

$$\boldsymbol{x}_o(t) \equiv \sum_{k=-\infty}^{\infty} \boldsymbol{d}_k u_o(t - k/B) \quad B = N/T_o$$

is periodic, with period T_o, and its Fourier series is given by

$$\boldsymbol{x}_o(t) \equiv \sum_{k=-\infty}^{\infty} \boldsymbol{X}_k \cdot e^{j2\pi kBt}$$

$$\boldsymbol{X}_m \equiv \frac{1}{T}\int_o^{T_0} \boldsymbol{x}_o(t) \cdot e^{-j2\pi mBt} dt = \frac{B}{N}\sum_{k=0}^{N-1} \boldsymbol{d}_k \cdot e^{-j2\pi km/N} = B \cdot \boldsymbol{D}_m \, . \tag{A.1}$$

The signal $\boldsymbol{x}_o(t)$ is filtered by the transfer function $\Pi(f)$ and it is multiplied by a time window $w(t)$ to produce $\boldsymbol{x}(t)$ [see Equation (1)]

$$\boldsymbol{x}(t) = w(t) \cdot \boldsymbol{x}_o(t) * \mathit{rect}(t)$$

$$w(t) \equiv \begin{cases} 1 & -T_g \le t < T_o \\ 0 & \text{elsewhere} \end{cases}$$

Then, the signal $\boldsymbol{x}(t)$ is filtered by $\boldsymbol{H}_{BT}(f) \cdot \boldsymbol{H}_T(f) \cdot \boldsymbol{H}_R(f) \equiv \boldsymbol{H}(f) \Leftrightarrow \boldsymbol{h}(t)$, to produce $\boldsymbol{y}(t) = \int_0^{\delta} \boldsymbol{h}(\tau) \cdot \boldsymbol{x}(t-\tau) \cdot d\tau$ [see Equation (5): δ is the duration of the impulse response]. Finally, $\boldsymbol{y}(t)$ is sampled at frequency B and FFT processed. We observe that $\boldsymbol{y}(t)$ can be interpreted as a sum (integral) of copies of $\boldsymbol{x}(t)$, each delayed by τ and multiplied by $\boldsymbol{h}(\tau)\cdot d\tau$; therefore, if the duration δ of $\boldsymbol{h}(t)$ is lower than T_g, in the previous integral the windowing of $\boldsymbol{x}(t)$ can be obviously eliminated, and $\boldsymbol{y}(t)$ becomes periodic, with period T_o. We have

$$\boldsymbol{y}(t) \equiv \sum_{k=-\infty}^{\infty} \boldsymbol{Y}_k \cdot e^{j2\pi kBt/N} \quad \boldsymbol{Y}_m \equiv B \cdot \boldsymbol{D}_m \cdot \boldsymbol{H}(f_m)$$

and finally

$$\begin{aligned} \boldsymbol{D}^{\wedge}_m &\equiv \frac{1}{N}\sum_{n=0}^{N-1} \boldsymbol{y}(n/B) \cdot e^{j2\pi nm/N} = \frac{1}{N}\sum_{n=0}^{N-1}\sum_{k=-\infty}^{\infty} \boldsymbol{Y}_k \cdot e^{j2\pi(k-m)\cdot n/N} = \\ &= \frac{1}{N}\sum_{k=-\infty}^{\infty} \boldsymbol{Y}_k \sum_{n=0}^{N-1} e^{j2\pi(k-m)\cdot n/N} = \boldsymbol{Y}_m = B \cdot \boldsymbol{D}_m \cdot \boldsymbol{H}(f_m) \end{aligned} \tag{Q.E.D.}$$

Appendix B

The values of $\boldsymbol{p}$ can be written as $\boldsymbol{p} = e^{j\xi}$, $\xi = \pm 45°, \pm 135$. Thus, from (10): $\boldsymbol{p}_m^\wedge = b_m e^{j(\xi+\varphi_m)} + \nu_m$, and, on the real axis

$$p_{c,m}^\wedge \equiv \mathrm{Re}\{\boldsymbol{p}_m^\wedge\} = \frac{b_m}{\sqrt{2}}(\pm\cos\varphi_m \pm \sin\varphi_m) + \nu_{c,m}\ ,$$

where $\nu_{c,m}$ is a gaussian noise component with zero mean and variance $\sigma_\nu^2/2$.

Therefore, the bit error probability on the real axis is the probability of the following two mutually exclusive events

$$\mathtt{E}^+ :\ \nu_{c,m} > \frac{b_m}{\sqrt{2}}(\cos\varphi_m + \sin\varphi_m) \equiv x_m$$
$$\mathtt{E}^- :\ \nu_{c,m} > \frac{b_m}{\sqrt{2}}(\cos\varphi_m - \sin\varphi_m) \equiv y_m$$

with probability

$$Prob\{\mathtt{E}^+\} = \frac{1}{2} erfc\left\{\frac{x_m}{\sqrt{2}(\sigma_v/\sqrt{2})}\right\} \quad \text{and} \quad Prob\{\mathtt{E}^-\} = \frac{1}{2} erfc\left\{\frac{y_m}{\sqrt{2}(\sigma_v/\sqrt{2})}\right\}$$

respectively. Therefore, the average bit error probability on the real axis is given by

$$P_{c,m} \equiv \frac{1}{2}(Prob\{\mathtt{E}^+\} + Prob\{\mathtt{E}^-\})\ .$$

Obviously, the same formula holds for the imaginary axis, which demonstrates Equation (11).

Maria-Gabriella Di Benedetto was born in Naples, Italy, in 1958. She obtained her “Laurea” in electrical engineering from the University of Rome “La Sapienza” in 1981, magna cum laude and publication of her thesis. She went on to specialize in control systems engineering (1983) and earned her “Dottore di Ricerca” (Ph.D.) in electrical communications also from the University of Rome “La Sapienza” in 1987.

Her professional positions have included numerous fellowships and Associate professorships – she is presently an associate professor of Electrical Communications at the University of Rome “La Sapienza” – and various visiting positions, at Massachusetts Institute of Technology (Cambridge, U.S.A.), and University of California at Berkeley (U.S.A.). In 1994, she received the Mac Kay professorship academic award, at the University of California at Berkeley (U.S.A.). Her research interests include speech analysis and synthesis, and the design of future generation wireless telecommunication systems. She currently plays an active role in the Advanced Communications Technologies and Services (ACTS) program of the European Union, as project manager for the University of Rome “La Sapienza” of three projects focused on standardization of future mobile telecommunication systems.

Dr. Di Benedetto is a member of the Acoustical Society of America (ASA) and of the European Speech Communication Association (ESCA).

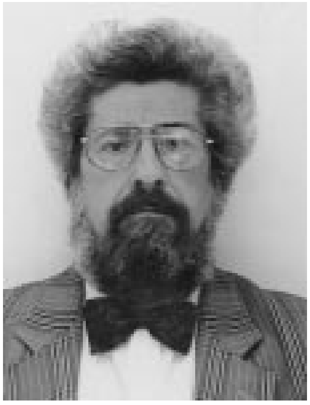

Paolo Mandarini was born in Rome in 1940. He received his “Laurea” degree in electronic engineering from the University of Rome in 1963.

From 1965 to 1971, he was a research fellow at the Fondazione Ugo Bordoni, Rome. In 1971, he joined the INFOCOM department of the University of Rome “La Sapienza” where he is currently Full professor of Electrical Communications. Professor Mandarini’s research activities are in the field of signal theory, detection theory and related topics, with emphasis in digital communications and speech analysis.